Longitudinal single-cell transcriptomics reveals distinct patterns of resistance in acute myeloid leukemia

Yanan Zhai *et al*.

Supplemental Methods

AML samples

In total, 6 paired Dx-Re bone marrow aspirates from adult AML patients, aged between 31 and 69 and diagnosed with *AML1-ETO* (n=2 low risk cases) or *FLT3*-ITD (n=1 intermediate and n=3 high risk) were analyzed from the AMLSG BiO Registry study (NTC 01252485). The phenotypic characterization (*AML1-ETO* and *FLT3*-ITD) was performed at the reference laboratory of the German and Austrian AML Study Group (AMLSG). All patients received intensive standard induction chemotherapy with cytarabine and an anthracycline (7+3 regimen) followed by high-dose cytarabine consolidation cycles. Patient characteristics are summarized in **Supplementary Table S1**. Informed consent for both treatment and biobanking of leukemia samples according to the Declaration of Helsinki was given by all patients. Approval was obtained from the ethical review board of the University of Ulm (Ethikkommission der Universität Ulm).

Cell preparation

Bone marrow aspirates from AML patients were processed using density gradient centrifugation to isolate mononuclear cells, viably frozen in medium containing 10% DMSO and shipped with dry ice. Cryopreserved AML samples were thawed at 37℃. After washing with cold PBS, cells were resuspended in 500µl PBS with 0.2% human serum and incubated for 10 minutes on ice. After centrifugation and removing the supernatant, cells were resuspended in 200µl cold PBS with 20µl PE-conjugated CD33 and 20µl APC-conjugated CD34 (eBioscience). Cells were stained for 30 minutes on ice, washed with cold PBS with 0.5% BSA and resuspended in 500µl PBS with 0.5% BSA and 1µl 7-AAD (eBioscience). After incubation for 10 minutes, CD33/CD34+ cells were sorted into 384-well plate (BioRad) containing well-specific primers (100nl, 0.75pmol/µl) and 5µl mineral oil (Sigma-Aldrich) on the BD FACS Aria cell sorter. After sorting plates were sealed and span down for 2 minutes at 2000g, snap frozen on dry ice and stored at -80℃ until use.

Single cell SORT-seq

We applied SORT-seq[1], a method that integrates single cell FACS sorting (Fluorescence-Activated Cell Sorter) with the CEL-Seq2 protocol[2] to measure gene expression at single cell resolution. External RNA Controls Consortium (ERCC) transcripts were spiked-in to detect empty wells, low quality mRNA and failed reactions. The frozen plates were centrifuged at 1400 RPM for 2 minutes at 4°C before processing. Processing of single cell plates included

36 first strand synthesis and barcoding in the 384 well plate. mRNA from the single cells were
37 pooled and batch amplified by in vitro transcription (IVT) (Invitrogen # AM1334). Sequence
38 libraries were prepared with Phusion High-Fidelity Polymerase (NEB).

39 **Bulk RNA-seq**

40 Total RNA was extracted using Quick-RNA Microprep Kit (Zymo Research) according to the
41 manufacturer protocol with DNaseI treatment. The RNA concentration was quantified with
42 Qubit Fluorometer (Invitrogen). RNA libraries were prepared with KAPA RNA HyperPrep Kit
43 with RiboErase (HMR) kit (Roche) following the manufacturer's recommendations. RNA-
44 seq libraries were paired-end sequenced on an Illumina Nextseq 500 at an average depth
45 of ~30M reads.

46 **Detection of *FLT3*-ITD at diagnosis and relapse**

47 The presence of *FLT3*-ITD was detected by DNA-based PCR followed by capillary
48 electrophoresis. The detailed procedures were described previously[3].

49 Data analysis

50 **Sequencing and mapping**

51 Single cell libraries were pair-end sequenced on an Illumina NextSeq500 at an average
52 depth of ~30M reads per library and demultiplexed using bcl2fastq version 2.15.0.4 with
53 default settings. We used STAR version 2.7.2b[4] to map the 42nt long read1 to human
54 reference genome hg38. Next, we used UMI-tools[5] to reconstruct the gene by cell UMI
55 count matrix from the BAM file.

56 **Normalization, dimensionality reduction and cluster analysis**

57 We used the Seurat v3[6] R-package for downstream analysis. First, low quality cells (genes
58 detected < 500 or UMI count > 12,000 or mitochondrial UMIs > 30% or ERCC reads > 20%)
59 were discarded (**Supplementary Fig. 1A)**. Ribosomal and mitochondrial genes were also
60 discarded prior to normalization. Cells from all libraries were concatenated and $\log_2$
61 normalized. Next, we applied principal component analysis (PCA) on the 2,000 most
62 variable genes to reduce the dimensionality of the dataset and retained the 50 components
63 for cluster analysis and the identification of marker genes. Cluster analysis was run using
64 the Louvain algorithm. Cluster markers were identified using the Seurat function
65 *FindAllMarkers* with parameters *min.pct*=0.25, *logfc.threshold*=0.5 and *only.pos*=FALSE.
66 Marker genes discriminating two clusters or Dx from Re cells were obtained usng the
67 Seurat function *FindMarkers* with parameters *min.pct*=0.25, *logfc.threshold*=0.5,
68 *min.diff.pct*=0.2 and *only.pos*=FALSE. All marker genes with adjusted p-value > 0.01 were
69 discarded.

70 **Whole exome sequencing analysis**

We used the GATK toolkit version v4.2.0[7] to detect short somatic variants following the GATK best practices workflows "*Data pre-processing for variant discovery*" and "*Somatic short variant discovery (SNVs + Indels)"* with small modifications. Briefly, paired-end reads were aligned using BWA version 2.2.1[8], discarding reads with MAPQ < 20. PCR duplicates were marked using Sambamba 0.8.0 *markdup*[9] and base quality scores were recalibrated using the GATK functions *BaseRecalibrator* and *ApplyBQSR* . Variants were called using the *panel of normals* (PON) and *gnomAD* VCF file provided in the GATK resource bundle in two modes: Dx and Re as tumor samples and Cr as a germline control, or all three samples as tumor only. The rationale for this approach is that variants present (at low frequency) in the Cr sample (due to minimal residual disease) are sometimes discarded as germline. Variants were filtered with *FilterMutectCalls* and annotated with the Ensembl Variant Effect Predictor (VEP) version 104[10].

Variants were discarded when ANY of the following conditions were satisfied:

- The variant FILTER status was unequal to "PASS" or "slippage."
- The variant had less than 5 reads on the alternative allele (AD < 5) in the Dx, Re and Cr samples;
- The variant allele frequency was below 0.05 (VAF < 0.05) in the Dx, Re and Cr samples;
- The variant had a gnomAD allele frequency $\geqslant 1.0 \times 10^{-3}$;
- The variant allele frequency did not change significantly between Dx vs CR or Re vs CR (p-adjusted $\geqslant$ 0.01; Fisher's exact test)
- The variant allele frequency at Cr exceeded 0.2 ($VAF_{CR} > 0.2$)

Mutations were visualized using the *maftools* R-package[12] and listed in supplemental table 2.

References

1. Muraro MJ, Dharmadhikari G, Grün D, et al. A Single-Cell Transcriptome Atlas of the Human Pancreas. *Cell Syst*. 2016;3(4):385-394.e3. doi:10.1016/j.cels.2016.09.002

2. Hashimshony T, Senderovich N, Avital G, et al. CEL-Seq2: Sensitive highly-multiplexed single-cell RNA-Seq. *Genome Biol*. 2016;17(1):1-7. doi:10.1186/s13059-016-0938-8

3. Schmalbrock LK, Dolnik A, Cocciardi S, et al. Clonal evolution of acute myeloid leukemia with FLT3-ITD mutation under treatment with midostaurin. *Blood*. 2021;137(22):3093-3104. doi:10.1182/blood.2020007626

4. Dobin A, Davis CA, Schlesinger F, et al. STAR: Ultrafast universal RNA-seq aligner. *Bioinformatics*. 2013;29(1):15-21. doi:10.1093/bioinformatics/bts635

5. Smith T, Heger A, Sudbery I. UMI-tools: modeling sequencing errors in Unique Molecular Identifiers to improve quantification accuracy. *Genome Res*. 2017;27(3):491-499. doi:10.1101/GR.209601.116

108 6. Stuart T, Butler A, Hoffman P, et al. Comprehensive Integration of Single-Cell Data. *Cell*.
109 2019;177(7):1888-1902. doi:10.1016/j.cell.2019.05.031

110 7. Genomics in the Cloud: Using Docker, GATK, and WDL in Terra - Geraldine A. Van der
111 Auwera, Brian D. O'Connor - Google Boeken.

112 8. Md V, Misra S, Li H, Aluru S. Efficient architecture-aware acceleration of BWA-MEM for
113 multicore systems. *Proc - 2019 IEEE 33rd Int Parallel Distrib Process Symp IPDPS 2019*.
114 Published online May 2019:314-324. doi:10.1109/IPDPS.2019.00041

115 9. Tarasov A, Vilella AJ, Cuppen E, Nijman IJ, Prins P. Sambamba: fast processing of NGS
116 alignment formats. *Bioinformatics*. 2015;31(12):2032-2034.
117 doi:10.1093/BIOINFORMATICS/BTV098

118 10. McLaren W, Gil L, Hunt SE, et al. The Ensembl Variant Effect Predictor. *Genome Biol*.
119 2016;17(1). doi:10.1186/S13059-016-0974-4

120 11. Benjamini Y, Hochberg Y. Controlling the False Discovery Rate: A Practical and Powerful
121 Approach to Multiple Testing. *J R Stat Soc Ser B*. 1995;57(1):289-300.
122 doi:10.1111/j.2517-6161.1995.tb02031.x

123 12. Mayakonda A, Lin D-C, Assenov Y, Plass C, Koeffler HP. Maftools: efficient and
124 comprehensive analysis of somatic variants in cancer. *Genome Res*. 2018;28(11):1747-
125 1756. doi:10.1101/GR.239244.118

126

Supplemental Figure Legends

Supplemental Figure 1. Quality Control of single cell data. (A) Violin plots depicting the detected number of genes (top) and unique transcripts (bottom) per cell. (B) Venn diagram showing the number of DEGs between the Dx and Re sample, for a pairwise comparison in the four *FLT3*-ITD patients. Very few DEGs are shared between patients. (C) Same as (B), for the two *AML1-ETO* patients.

Supplemental Figure 2. Single cell landscape of Single cell landscape of *FLT3*-ITD patient s232. (A) UMAP of Dx and Re cells for *FLT3*-ITD patient s232 colored by timepoint (top) or cell cluster (bottom). (B) Heatmap displaying the top 20 cluster marker genes. Color represents row normalized expression values. (C) Overrepresented GO terms (category: biological pathway) in cluster 1 (Dx) and 3 (Re). P-values: hypergeometric test (BH-corrected). (D) Gene expression of selected mTORC1 pathway members.

Supplemental Figure 3. Single cell landscape of *FLT3*-ITD patient s292. (A) UMAP of Dx and Re cells for *FLT3*-ITD patient s292 colored by timepoint (top) or cell cluster (bottom). (B) Heatmap displaying the top 20 cluster marker genes. Color represents row normalized expression values. (C) overrepresented GO terms (category: biological pathway) per cluster.

Supplemental Figure 4. Single cell landscape of *FLT3*-ITD patient s2275. (A) UMAP of Dx and Re cells for *FLT3*-ITD patient s2275 colored by timepoint (top) or cell cluster (bottom). (B) Heatmap displaying the top 20 cluster marker genes. Color represents row normalized expression values. (C) overrepresented GO terms (category: biological pathway) for clusters 1 (Dx) and 5 (Re).

Supplemental Figure 5. Relapse cells of *FLT3*-ITD patient s3432 are associated with exocytosis. (A) Gene expression of selected RAS-pathway members. (B) overrepresented GO terms (category: biological pathway) for clusters 4. (C) Selected genes associated with exocytosis. Color depicts relative expression; size depicts the relative number of cells for a which at least one transcript was detected. ** $p < 0.01$, *** $p < 0.001$, Wilcox rank sum / Mann-Whitney U test.

Supplemental Figure 6. Cells in cluster 6 (blue circle, s914 *AML1-ETO*) simultaneously express hematopoietic stem-/progenitor- (*CD34*), monocyte (*LYZ*), B-cell (*MS4A1*), erythrocyte (*HBB*) and cell cycle (*TOP2A, MKI67*) marker genes. This indicates that these cells are doublets or contaminated by ambient RNA and were discarded from further analysis. Color bar represents the expression level of corresponding genes.

Supplemental Figure 7. Single cell landscape of *AML1-ETO* patient s220. (A) Heatmap displaying the top 20 cluster marker genes. Color represents row normalized expression values. Marker genes shared between cluster 4 (Dx) and 5 (Re) are highlighted inside a black rectangle. (B) overrepresented GO terms (category: biological pathway) at Dx and Re.

163 ## Supplemental Table Legends

164 **Supplemental Table1.** Clinical information and sequencing details of the patients

165 **Supplemental Table2.** Dynamic changes of mutations between Dx and Re (WES) and
166 detected fusion genes from bulk RNA-Seq. Please see the individual Excel table.

167 **Supplemental Table3.** Characterization of *FLT3*-ITD at diagnosis and relapse.

168 **Supplemental Figure 1.**

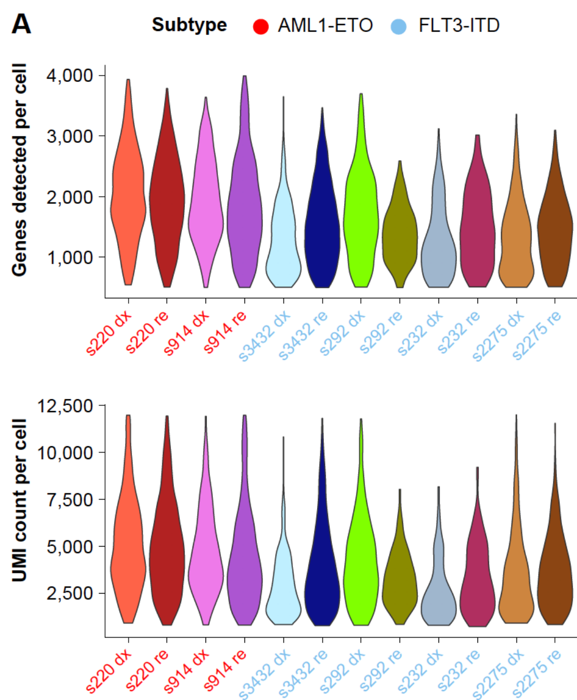

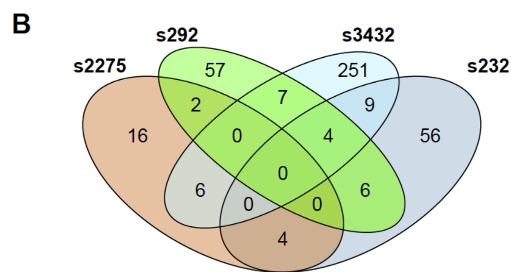

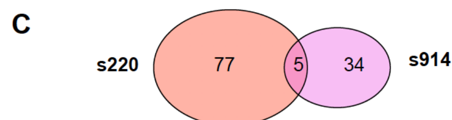

169

170 **Supplemental Figure 2 (s232).**

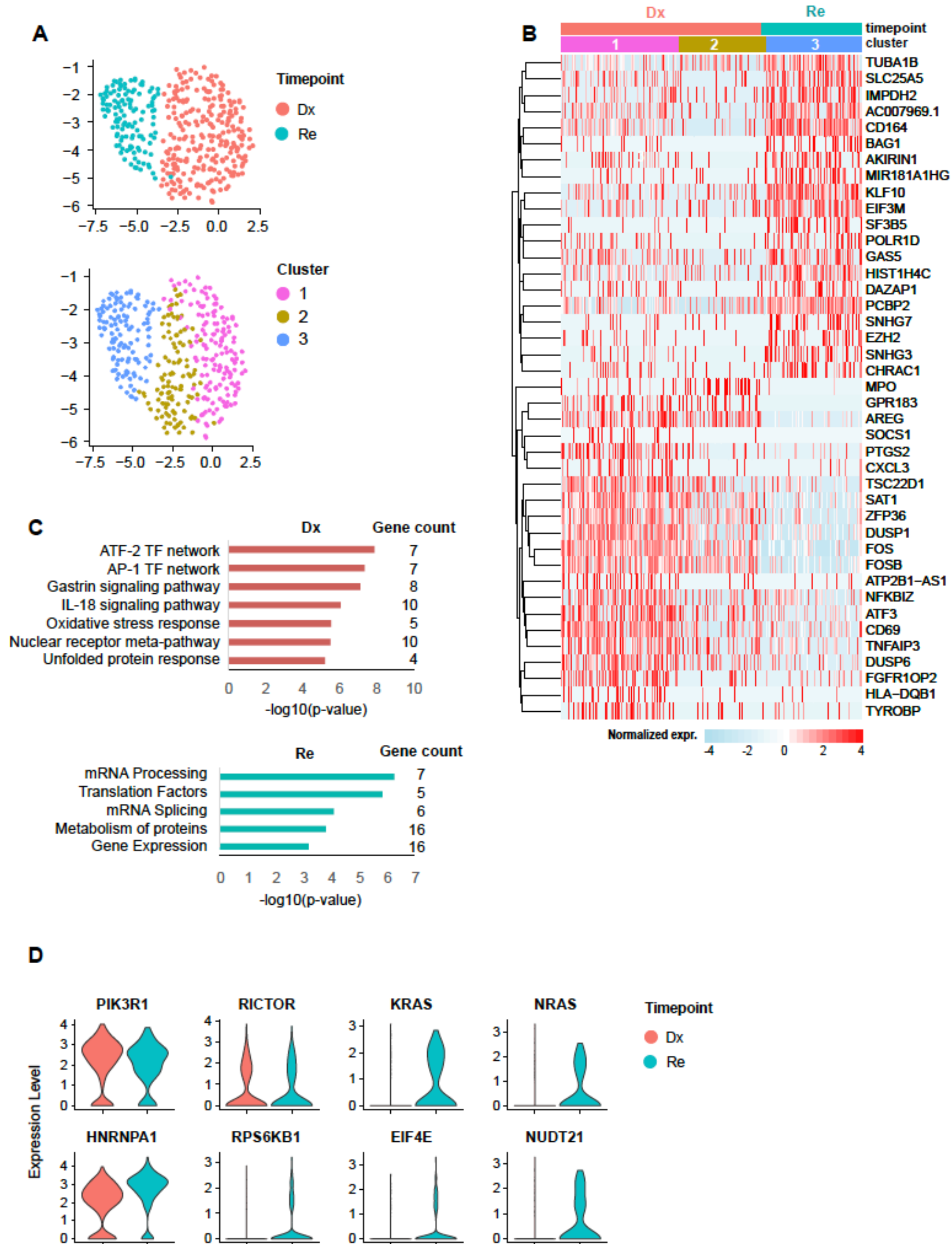

171

172

173 **Supplemental Figure 3 (s292).**

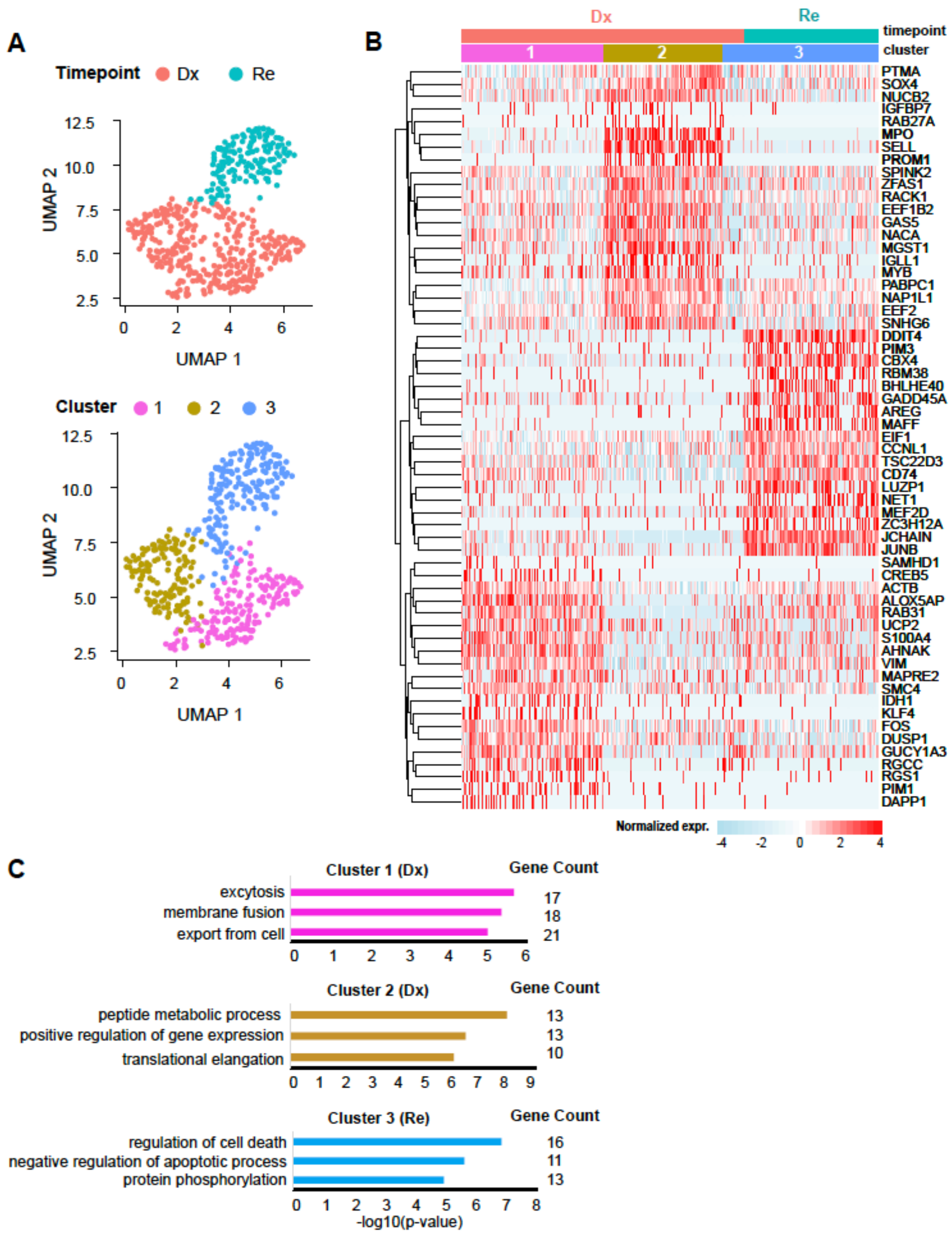

174

175

176 **Supplemental Figure 4 (s2275).**

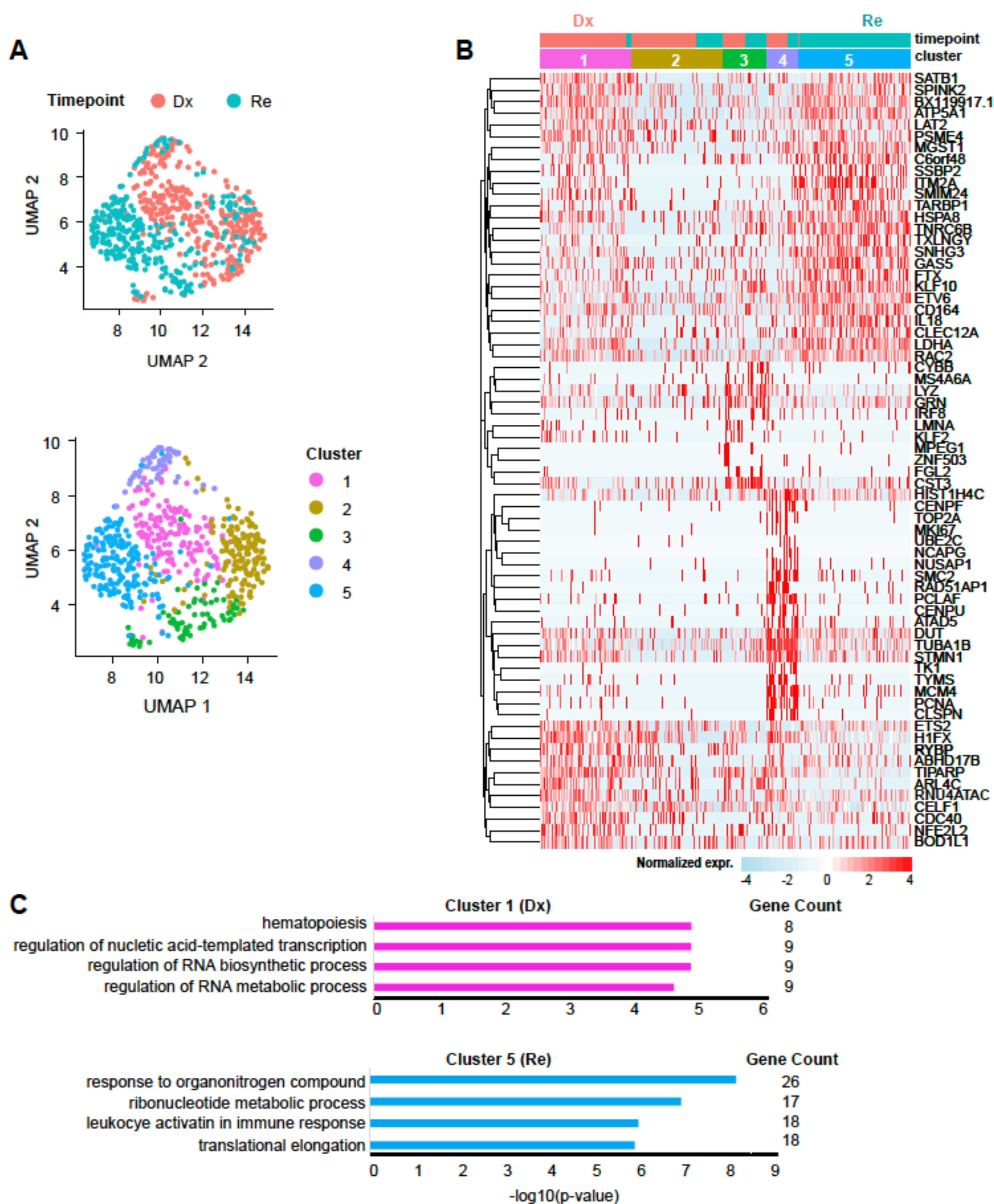

177

178 **Supplemental Figure 5 (s3432).**

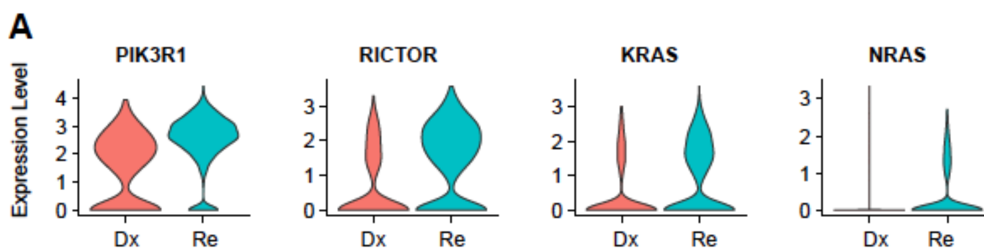

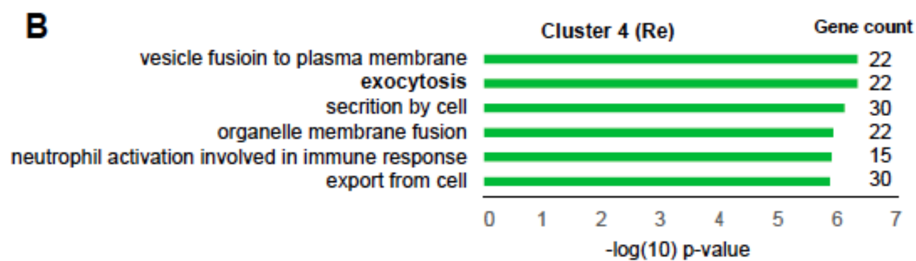

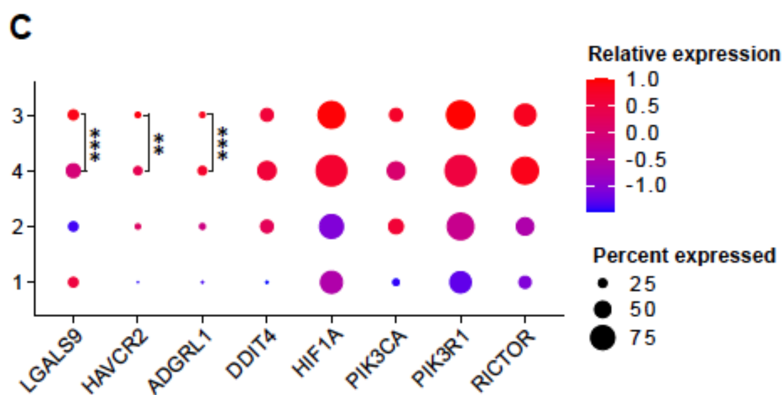

179

180

181 **Supplemental Figure 6 (s914).**

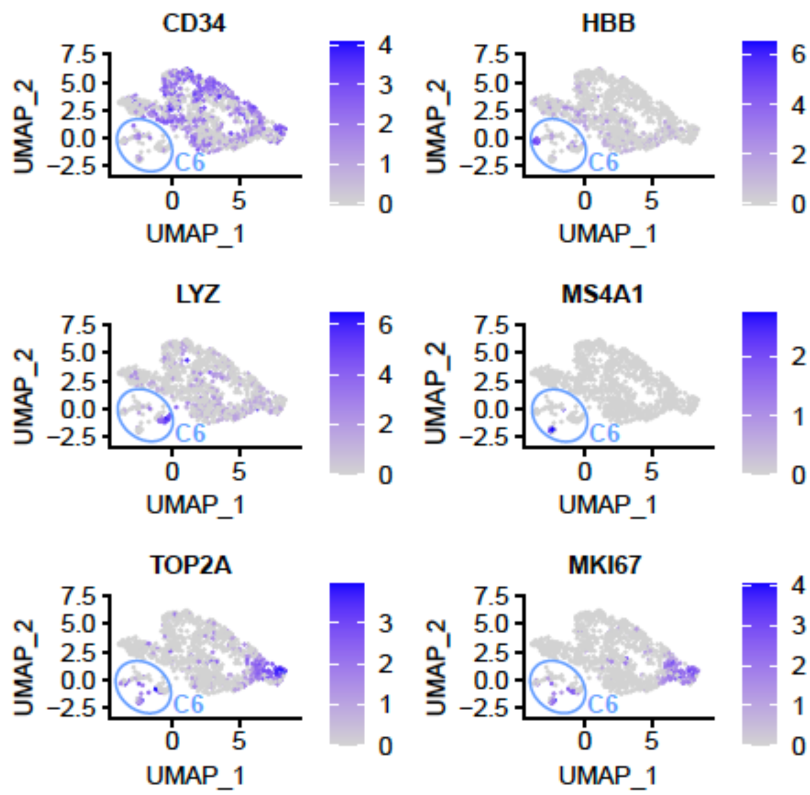

182

183

184 **Supplemental Figure 7 (s220).**

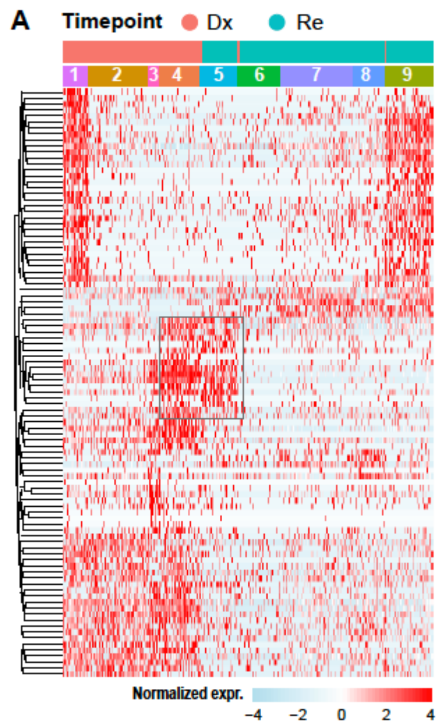

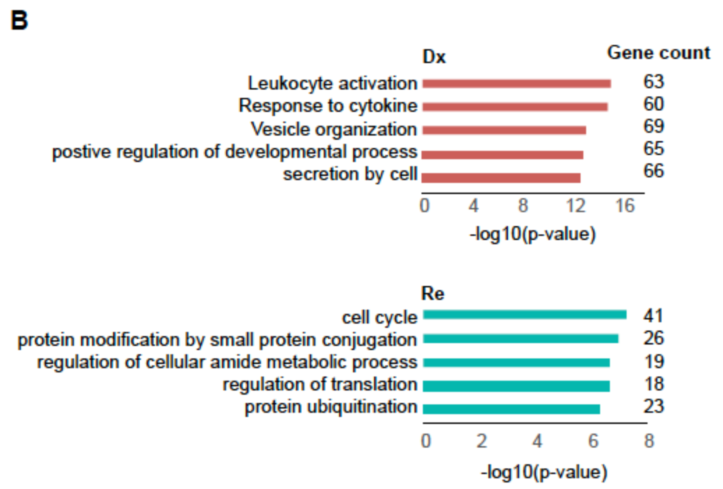

185

186

187 ## Supplemental Tables

188 **Supplemental Table1.** Clinical information and sequencing details of the patients

Patient ID	Gender	Age	Sample Source		Blast%		Enrichment	
			Dx	Re	Dx	Re	Dx	Re
s220 *AET1-ETO*	Male	57	BM	BM	90%	NA	CD34	CD34
s914 *AML1-ETO*	Male	31	BM	BM	30%	NA	CD34	CD34
s232 *FLT3*-ITD	Male	53	BM	BM	80%	90%	CD34	CD34
s292 *FLT3*-ITD	Male	50	BM	BM	90%	60%	CD34	CD34
s2275 *FLT3*-ITD	Male	33	BM	BM	95%	95%	CD34	CD34
s3432 *FLT3*-ITD	Female	66	BM	BM	95%	91%	CD33	CD34

189

Patient ID	Cell number after QC		Counts per cell (Mean)		Features per cell (Mean)	
	DX	Re	DX	Re	DX	Re
s220 *AML1-ETO*	576	929	5 112	4 856	2 042	1 939
s914 *AML1-ETO*	314	688	4 713	4 411	1 951	1 851
s232 *FLT3*-ITD	249	123	2 653	3 289	1 278	1 497
s292 *FLT3*-ITD	324	152	4 224	3 261	1 726	1 380
s2275 *FLT3*-ITD	309	281	3 530	3 681	1 328	1 457
s3432 *FLT3*-ITD	509	1 158	2 895	3 956	1 299	1 563

190 BM: Bone Marrow; NA: not available

191 **Supplemental Table3.** Characterization of *FLT3*-ITD at diagnosis and relapse.

Patient ID	Time point	FLT3-ITD allelic ratio	ITD same Dx/Rel 1=yes, 0=no	ITD loss (=FLT3-ITD negative at rel) 1=yes, 0=no	ITD change at rel 1=yes, 0=no	switch (insertion site, length) 1=yes, 0=no	loss of min 1 clone at rel 1=yes, 0=no	gain of min 1 clone at rel 1=yes, 0=no
s232	Dx	0,398						
	Re	0,744	0	0	1	0	1	0
s292	Dx	0,659						
	Re	0,71	0	0	1	1	0	0
s2275	Dx	0,988						
	Re	26,312	0	0	1	1	0	0
s3432	Dx	0,617						
	Re	0,325	1	0	0	0	0	0

192